have been described in many cell types (*21*). It is likely that type I myosins play an important role in endocytic internalization via these pathways.

REFERENCES AND NOTES

1. T. Hasson and M. S. Mooseker, *Curr. Opin. Cell Biol.* **7**, 587 (1995).
2. R. E. Cheney and M. S. Mooseker, *ibid.* **4**, 27 (1992); J. A. Hammer, *J. Muscle Res. Cell. Motil.* **15**, 1 (1994).
3. H. V. Goodson and J. A. Spudich, *Cell Motil. Cytoskeleton* **30**, 73 (1995).
4. W. M. Bement, T. Hasson, J. A. Wirth, R. E. Cheney, M. S. Mooseker, *Proc. Natl. Acad. Sci. U.S.A.* **91**, 6549 (1994).
5. J. L. Tan, S. Ravid, J. A. Spudich, *Annu. Rev. Biochem.* **61**, 721 (1992).
6. W. M. Bement, J. A. Wirth, M. A. Mooseker, *J. Mol. Biol.* **243**, 356 (1994); H. E. Stöffler, C. Ruppert, J. Reinhard, M. Bähler, *J. Cell Biol.* **129**, 819 (1995).
7. I. C. Baines, A. Corigliano-Murphy, E. D. Korn, *J. Cell. Biol.* **130**, 591 (1995). K. D. Novak, M. D. Peterson, M. C. Reedy, M. A. Titus, *ibid.* **131**, 1205 (1995).
8. M. I. Geli and H. Riezman, data not shown.
9. *MYO3* and *MYO5* were deleted in the same diploid to obtain a heterozygotic strain, RH3375 (*MATa/MATα ade2/ADE2 his3/his3 myo3Δ::HIS3/MYO3 myo5Δ::TRP1/MYO5 leu2/leu2 lys2/LYS2 trp1/trp1 ura3/ura3 bar1/bar1*). From this strain the RH3376, RH3377, and RH3378 strains were generated by tetrad dissection (Table 1). Deletion of *MYO3* has been described (*6*). For deletion of *MYO5*, the fragments Eco RI–Hind III and Pst I–Bgl II (Fig. 1A) were used to flank a 0.9-kb DNA fragment carrying the *TRP1* gene. The spores were analyzed by replica plating on synthetic dextrose medium lacking the corresponding amino acids. None of the predicted double mutants (*TRP1 HIS3*) out of 20 dissected tetrads formed colonies. A double mutant harboring plasmid pmyo5-1 or pMYO5 (*13*) was able to form pinpoint-sized colonies upon plasmid loss. When the pmyo5-1–carrying strain was shifted to 37°C, the proportion of unbudded cells did not change.
10. E. Kübler and H. Riezman, *EMBO J.* **12**, 2855 (1993); E. Kübler, F. Schimmöller, H. Riezman, *ibid.* **13**, 5539 (1994).
11. V. Dulić *et al.*, *Methods Enzymol.* **194**, 697 (1991).
12. E511 (Glu511) of Myo2p in the putative actin binding domain [G. C. Johnston, J. A. Pendergast, R. A. Singer, *J. Cell Biol.* **113**, 539 (1991)] corresponds to E472 (Glu472) in Myo5p (Fig. 1A). The allele E472K (Glu472 → Lys472) (*myo5-1*) was generated by PCR and cloned into a centromere-based plasmid [YCplac33; *Gene* **74**, 527 (1988)] to generate pmyo5-1. Wild-type *MYO5* was also cloned into YCplac33 to generate pMYO5.
13. RH3380, RH3383, RH3382, and RH3384 strains (Table 1) were generated by tetrad dissection from RH3375 (*9*) transformed with pmyo5-1 or pMYO5 (*12*). RH3382 and RH3384 were used as controls for strains RH3380 and RH3383 in order to guarantee similar amounts of expression of WT and ts Myo5p. Strains RH3382 and RH3384 behaved in all experiments exactly as did the RH3376 strain, except for α-factor uptake at 37°C, where the initial uptake rates were reduced by approximately 25%.
14. L. Hicke, B. Zanolari, M Pypaert, H. Riezman, in preparation.
15. C. A. McGoldrick, C. Gruver, G. S. May, *J. Cell. Biol.* **128**, 577 (1995).
16. T. S. Stevens, B. Esmon, R. Schekman, *Cell* **30**, 439 (1982).
17. S. Raths, J. Rohrer, F. Crausaz, H. Riezman, *J. Cell Biol.* **120**, 55 (1993).
18. J. Mulholland *et al.*, *ibid.* **125**, 381 (1994).
19. H. Benedetti, S. Raths, F. Crausaz, H. Riezman, *Mol. Biol. Cell* **5**, 1023 (1994); A. L. Munn, B. J. Stevenson, M. I. Geli, H. Riezman, *ibid.* **6**, 721 (1995).
20. *myo2*-66 (10), *tpm1Δ*, *pfy1Δ* (19) strains disrupt the actin cytoskeleton but are not required for endocytosis.
21. C. Lamaze and S. L. Schmid, *Curr. Opin. Cell. Biol.* **7**, 573 (1995); M. Maniak, R. Rauchenberger, R. Albrecht, J. Murphy, G. Gerisch, *Cell* **83**, 915 (1995); K. Sandvig and B. Van Deurs, *J. Biol. Chem.* **265**, 6382 (1990); T. A. Gottlieb, I. E. Ivanov, M. Adesnik, D. D. Sabatini, *J. Cell Biol.* **120**, 695 (1993); G. Jung and J. A. Hammer III, *ibid.* **110**, 1955 (1990).
22. B. Zanolari., S. Raths, B. Singer-Krüger, H. Riezman, *Cell* **71**, 755 (1992).

23. We thank Riezman laboratory members for discussion; S. Schröder, A. L. Munn, A. Wesp, C. Sütterlin, and M. Schönbächler for critical reading of the manuscript; T. Aust and N. Stern for technical assistance; and H. Goodson for the plasmid to delete *MYO3*. Funded by a grant from the Swiss National Science Foundation (to H.R.). M.I.G. was supported by a European Molecular Biology Organization long-term fellowship.

19 December 1995; accepted 12 February 1996

Evaluating Electrostatic Contributions to Binding with the Use of Protein Charge Ladders

Jinming Gao, Mathai Mammen, George M. Whitesides*

Electrostatic interactions between charges on ligands and charges on proteins that are remote from the binding interface can influence the free energy of binding (ΔG_b). The binding affinities between charged ligands and the members of a charge ladder of bovine carbonic anhydrase (CAII) constructed by random acetylation of the amino groups on its surface were measured by affinity capillary electrophoresis (ACE). The values of ΔG_b derived from this analysis correlated approximately linearly with the charge. Opposite charges on the ligand and the members of the charge ladder of CAII were stabilizing; like charges were destabilizing. The combination of ACE and protein charge ladders provides a tool for quantitatively examining the contributions of electrostatics to free energies of molecular recognition in biology.

Although charged groups appear in a majority of biological molecules, and electrostatic interactions between these groups undoubtedly contribute energetically to many important biological interactions, it has been difficult to evaluate these contributions quantitatively. A recent, stimulating review of the influence of electrostatic interactions in biochemistry by Honig (*1*) analyzed this subject in detail and drew a number of startling inferences: for example, in some circumstances (*2, 3*), interactions between opposite charges may be destabilizing, rather than stabilizing as expected for idealized electrostatic interactions in vacuum (*4*).

Efforts to quantitate electrostatic effects in interactions of proteins with ligands have centered on proteins modified by site-specific mutagenesis (*5*). This technique, although powerful, is labor-intensive and is cumbersome when used to generate proteins that are multiply mutated. Here we summarize the energetics of interaction of the members of a protein charge ladder (*6*) derived from bovine carbonic anhydrase II (CAII) (E.C. 4.2.1.1, containing two isozymes of isoelectric points 5.4 and 5.9, respectively) (*7*) with benzenesulfonamides substituted in the para position with charged and neutral groups. CAII is a roughly spherical Zn(II) metalloenzyme with a conical binding pocket. This pocket is lined with both hydrophobic and polar residues but not with charged residues (*7*). The combination of affinity capillary electrophoresis (ACE) (*8*) and charge ladders derived from CAII and other proteins constitutes a versatile and convenient system with which to define electrostatic contributions to the energetics of the association of charged proteins and charged ligands.

Treatment of CAII with acetic anhydride generates a set of proteins in which distributions of positively charged Lys ε-ammonium groups are converted to neutral *N*-acyl derivatives (Eq. 1).

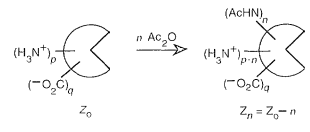

(1)

These sets of modified proteins appear in capillary electrophoresis (CE) as a set of evenly spaced peaks, which we call a "protein charge ladder" (*6*). In Eq. 1, n is the number of acylated amines [CAII has 18 Lys ε-NH_3^+, 26 Asp or Glu-CO_2^-, and 9 Arg-$NHC(NH_2)_2^+$ groups (*7*)], and Z_0 and Z_n are the charges of the native protein and proteins having n modified Lys groups, respectively. In CE, the electrophoretic mobility (μ_n) of a protein is proportional to its charge and inversely correlated with its molecular weight (M)

$$\mu_n \approx \frac{C_\Gamma}{M^\alpha} Z_n = \frac{C_\Gamma}{M^\alpha} Z_0 - \frac{C_\Gamma}{M^\alpha} n \qquad (2)$$

Department of Chemistry, Harvard University, 12 Oxford Street, Cambridge, MA 02138, USA.

*To whom correspondence should be addressed. E-mail: gwhitesides@gmwgroup.harvard.edu

where C_P is a proportionality constant that includes the influence of screening of charge by counterions in solution, and $\alpha \approx \frac{2}{3}$ for globular proteins (*9*, *10*). In the case of CAII, the families of acetylated derivatives differ in charge by integral units; they differ in molecular weight only minimally (the molecular weight of an acetyl group is 42 daltons; that of CAII is 30 kD). Therefore, all proteins with the same value of n have essentially the same electrophoretic mobility. ACE measures the changes in the mobility of the proteins in the charge ladder as a function of the concentration of a ligand in the electrophoresis buffer and yields the binding constant to each member of the charge ladder simultaneously (*8*).

We have determined binding constants for each member of the charge ladder of CAII (*11*) with seven structurally related ligands differing in charge and position of charge relative to the sulfonamide group (*12*) (Fig. 1). Scatchard analysis of the changes in electrophoretic mobility of each member of the CAII charge ladder with concentration of ligand yields its value of the binding constant K_b (*8*). Analysis of these data gives free energies of binding (ΔG_b) (Fig. 2).

We draw three conclusions from these data. First, acetylation of the Lys ε-amino groups of CAII does not influence its binding to neutral ligands (*13*): all members of the charge ladder bound ligands **2**, **3**, and **7** equally. This lack of discrimination suggests that the acetylated derivatives of CAII retain the native conformation at the active site, even when 16 $-NH_3^+$ groups are converted to -NHAc groups. Second, binding constants of the members of the charge ladder depend on the charge on the protein and the charge on the ligand in a regular way (*14*): the more negatively charged members of the charge ladder bound less tightly to a negatively charged ligand (**4**) and more tightly to a positively charged ligand (**1**) than did the less negatively charged members. Quantitatively, the magnitude of the dependence of ΔG_b on the net charge of CAII and its derivatives was $0.05Z_n$ to $0.1Z_n$ kcal mol^{-1} for the charged ligands **1** and **4** (*15*). Third, to a first approximation, the position of acetylation has little influence on the values of binding constants: the mobilities of all derivatives of CAII having the same overall charge (a single peak in the charge ladder) seemed to shift together as the concentration of the ligand increased. We believe that the small broadening of peaks in the center of the charge ladder (n = 6 to 12) reflects a slight heterogeneity in binding affinity within families of acylated derivatives of CAII having the same net charge.

The addition of one unit of negative charge to CAII stabilizes (or destabilizes) its interaction with ligand **1** (or **4**) by 0.05 to 0.1 kcal mol^{-1} (Fig. 2A). A simple, approximate, Coulombic model indicates that this value is physically reasonable. We model CAII as a spherical solid of radius r_0 = 20 Å (*16*) with a charge $Z_n = Z_0 - n$ [$Z_0 = -3.5$ at pH 8.3 (*17*)] distributed uniformly over its surface. We assume that the ionic strength of the solution is zero and that the dielectric constant outside the sphere is that of water ($\varepsilon = 80$); the model is independent of the value of ε inside the sphere. Bringing a test charge in from infinite distance (defined as being at potential energy $V = 0$) to a distance r (for $r \leq r_0$) results in a change $\Delta V \approx Z_n/4\pi\varepsilon\varepsilon_0 r_0 \approx 0.2Z_n$ kcal mol^{-1} (*10*), where ε_0 is the permittivity of free space; the observed value of $0.05Z_n$ to $0.1Z_n$ kcal mol^{-1} is consistent with this estimate (*18*). We are currently performing more rigorous calculations using Poisson-Boltzmann methods (*1*).

This electrostatic model of CAII-ligand interaction predicts that the magnitude of

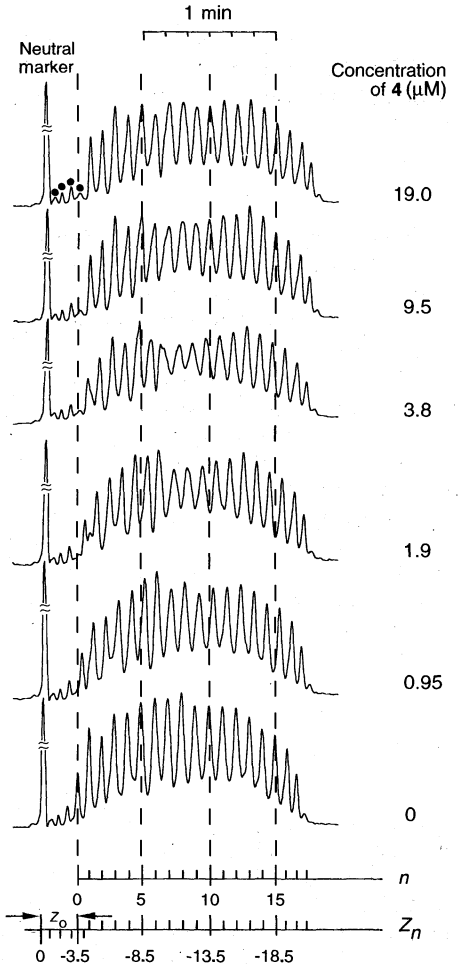

Fig. 1. Electropherograms of the binding of ligand **4** to the charge ladder of CAII. Increasing concentrations of ligand **4** in a buffer of 25 mM tris and 192 mM Gly (pH = 8.3) were used as the electrophoresis buffer. The neutral marker was 4-methoxybenzyl alcohol. The number of modified ε-amino groups (n) and net charge of the protein in the charge ladder ($Z_n = Z_0 - n$) are indicated below the electropherograms. The small peaks marked with (●) are impurities in the sample. Equivalent results were obtained for the other ligands.

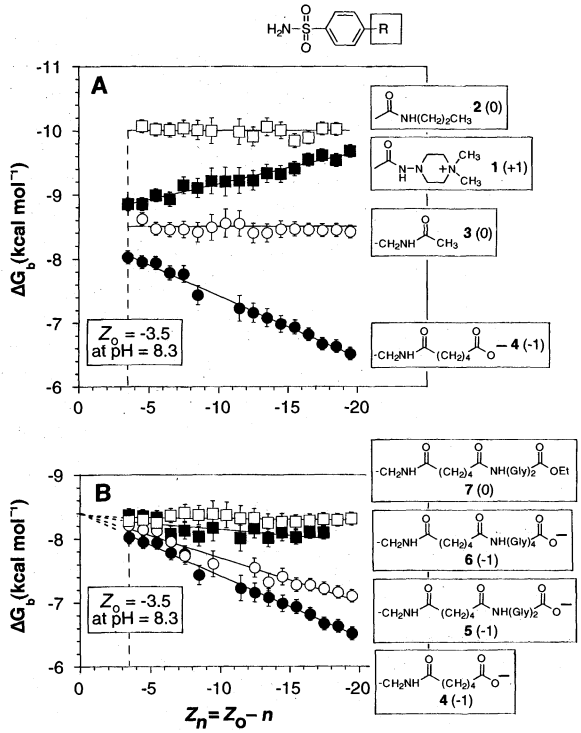

Fig. 2. Dependence of the free energy of binding (ΔG_b) on the charge of CAII (Z_n) in the charge ladder and on (**A**) the charge on the ligands (numbers in parentheses following the ligands indicate charge) and (**B**) the location of the charge relative to the sulfonamide group. The binding affinity of each member of the charge ladder to ligands **1** through **7** was measured by ACE in a buffer of 25 mM tris and 192 mM Gly (pH = 8.3). Because of slight broadening of the peaks near the center of the charge ladder (n = 6 to 12), the uncertainties in the values of ΔG_b for these derivatives are larger than those for the other parts of the charge ladder (for some values of n, the peak broadening resulted in missing data). The slopes ($\Delta\Delta G_b/\Delta Z$) from the linear regression analyses of ΔG_b versus Z_n yielded the magnitudes of influence of charges on CAII-ligand interactions. Values of $\Delta\Delta G_b/\Delta Z$ (in kilocalories per mole per charge) for these ligands: **1**, 0.05 ± 0.01; **2**, 0.01 ± 0.01; **3**, 0 ± 0.01; **4**, 0.10 ± 0.01; **5**, 0.07 ± 0.02; **6**, 0.02 ± 0.02; and **7**, 0 ± 0.01.

electrostatic interactions will decrease upon increase of the distance between the charged group on the ligand and the binding site of CAII. To test this hypothesis, we compared ligands **4**, **5**, and **6**, in which the negatively charged carboxylate group was separated from the sulfonamide group by increasing numbers of bonds (Fig. 2B). The dependence of free energy of binding on charge, $\Delta\Delta G_b/\Delta Z$, for ligands **4**, **5**, and **6** was 0.10 ± 0.01, 0.07 ± 0.02, and 0.02 ± 0.02 kcal mol^{-1} charge^{-1}, respectively. As expected, the interactions between the charges on ligands and proteins decreased as the number of bonds between the sulfonamide group and the charged group increased. The value of $\Delta\Delta G_b/\Delta Z$ for **4** is approximately twice that of the shorter ligand **1**; we have not established the origin of this difference.

Three characteristics of the combination of ACE and charge ladders are particularly useful for study of electrostatic contributions to the free energies of protein-ligand interactions. First, it generates large numbers of directly comparable data in a straightforward experimental system. Second, charge ladders can be generated from a large number of proteins, and although only certain charge ladders behave as simply as that from CAII, the technique has useful generality (*19*). Third, the technique readily permits quantitative evaluation of both intensive (ion composition and temperature) and extensive (ionic strength and pH) influences on the electrostatic contribution to biological interactions.

REFERENCES AND NOTES

1. B. Honig and A. Nicholls, *Science* **268**, 1144 (1995).
2. K. J. Lumb and P. S. Kim, *ibid.*, p. 436.
3. J. Novotny and K. Sharp, *Prog. Biophys. Mol. Biol.* **58**, 203 (1992).
4. The observation that interactions between colloidal particles of like charge can, in certain instances, be attractive further complicates our understanding of electrostatic effects in ionic media [N. Ise and H. Yoshida, *Acc. Chem. Res.* **29**, 3 (1996); K. S. Schmitz, *ibid.*, p. 7].
5. P. G. Thomas, A. G. Russell, A. J. Fersht, *Nature* **318**, 375 (1985).
6. J. Gao, F. A. Gomez, R. Haerter, G. M. Whitesides, *Proc. Natl. Acad. Sci. U.S.A.* **91**, 12027 (1994).
7. S. J. Dodgson, R. E. Tashian, G. Gros, N. D. Carter, Eds., *The Carbonic Anhydrases: Cellular Physiology and Molecular Genetics* (Plenum, New York, 1991).
8. Y.-H. Chu, L. Z. Avila, J. Gao, G. M. Whitesides, *Acc. Chem. Res.* **28**, 461 (1995).
9. S. K. Basak and M. R. Ladisch, *Anal. Biochem.* **226**, 51 (1995).
10. H. A. Abramson, L. S. Moyer, M. H. Gorin, *Electrophoresis of Proteins and the Chemistry of Cell Surfaces* (Reinhold, New York, 1942), chaps. 5 and 6.
11. The charge ladder of CAII was prepared as follows. The pH of three solutions of native CAII (0.1 mM in distilled water, 0.5 ml) was adjusted to pH 10 by addition of 0.1 N NaOH and was maintained at this value. Acetic anhydride (10, 20, and 40 equiv, respectively, 100 mM in dioxane) was added. After 30 min, the three solutions were mixed and diluted to 10 μM in a buffer of 25 mM tris and 192 mM Gly (pH = 8.3). This procedure gave a sample in which each member of the charge ladder could be easily analyzed. The neutral marker was 4-methoxybenzyl alcohol (50 μM).
12. We used a Beckman P/ACE 5500 system for CE. General conditions: operated at 15 kV; temperature T = 37°C, maintained by liquid cooling; capillary inner diameter, 50 μm; total length of capillary, 47 cm; length from inlet to detector, 40 cm. For the ACE experiments, different concentrations of a ligand were prepared in a buffer of 25 mM tris and 192 mM Gly (pH = 8.3). The capillary was flushed with 0.1 N NaOH, distilled water, and electrophoresis buffer for 2 min before each experiment.
13. Using competitive ACE (*8*), we measured the binding affinities of the neutral ligands **2** and **3** to CAII by competition with ligand **1** (+1 charge), and that of neutral ligand **7** by competition with ligand **5** (−1 charge).
14. A conventional fluorescence assay on samples containing mixtures enriched in low-Z_n and high-Z_n fractions of the charge ladder of CAII confirmed qualitatively the influence of its charge, and that of its ligands, on ΔG_b.
15. The lines that correlate ΔG_b with Z_n in Fig. 2 can be extrapolated to Z_n = 0. At this point, the influence of charge-charge interactions on binding should disappear. For ligands with the same structure inside the active site (Fig. 2B), the lines can be extrapolated to a common point (ΔG_b = −8.4 ± 0.1 kcal mol^{-1}) at Z_n = 0; for ligands with different structure inside the active site (Fig. 2A), the lines do not intersect at Z_n = 0, and therefore, other factors (for example, pK_a of sulfonamide groups or hydrophobic interactions) must contribute to differences in binding.
16. The dimensions of CAII taken from its crystal structure are 41 Å by 41 Å by 47 Å [A. Liljas *et al.*, *Nature* **235**, 131 (1972)].
17. We attribute the nonintegral net charge for CAII (Z_0 = −3.5) at pH 8.3 to the fractional protonation of charged residues such as His or water bound to Zn(II).
18. Dissolved salts should lower this calculated electrostatic cost further by partially screening the charges on CAII from those on ligands.
19. We have observed similar electrostatic effects on binding in three other systems. One comprises a monoclonal antibody, rat immunoglobulin IgG2b, interacting with differently charged synthetic ligands (ligand charges Z_L = −1, −3, −6, and −9) that contain a dinitrophenyl group. The observed free energy of binding correlated linearly with the charge on the ligand: $\Delta\Delta G_b/\Delta Z$ = 0.030 ± 0.006 kcal mol^{-1} charge^{-1}. The second system comprises vancomycin interacting with D-Ala–D-Ala; the observed value of $\Delta\Delta G_b/\Delta Z$ was 1.2 kcal mol^{-1} charge^{-1}. This larger value of electrostatic effect is consistent with a shorter distance between the two charged groups on vancomycin and the carboxylate group of D-Ala–D-Ala. The third system comprises a charge ladder of carboxypeptidase B interacting with Arg; the observed value of $\Delta\Delta G_b/\Delta Z$ was 0.05 ± 0.02 kcal mol^{-1} charge^{-1}. In all three systems, opposite charges stabilized the receptor-ligand complexes and like charges destabilized them. A number of proteins—including lysozyme, superoxide dismutase, peroxidase, dextranase, carboxypeptidase A, ribonuclease A, and papain—produce useful charge ladders on acetylation; we are using these ladders to examine electrostatic influences on binding their substrates or ligands.

20. This work was supported by NIH grant GM 51559. We thank J. Rao for helpful discussions and for the data involving vancomycin.

8 December 1995; accepted 12 March 1996

Adaptive Evolution of Human Immunodeficiency Virus–Type 1 During the Natural Course of Infection

Steven M. Wolinsky,*† Bette T. M. Korber,† Avidan U. Neumann, Michael Daniels, Kevin J. Kunstman, Amy J. Whetsell, Manohar R. Furtado, Yunzhen Cao, David D. Ho, Jeffrey T. Safrit, Richard A. Koup

The rate of progression to disease varies considerably among individuals infected with human immunodeficiency virus–type 1 (HIV-1). Analyses of semiannual blood samples obtained from six infected men showed that a rapid rate of CD4 T cell loss was associated with relative evolutionary stasis of the HIV-1 quasispecies virus population. More moderate rates of CD4 T cell loss correlated with genetic evolution within three of four subjects. Consistent with selection by the immune constraints of these subjects, amino acid changes were apparent within the appropriate epitopes of human leukocyte antigen class I–restricted cytotoxic T lymphocytes. Thus, the evolutionary dynamics exhibited by the HIV-1 quasispecies virus populations under natural selection are compatible with adaptive evolution.

In general, the natural history of HIV-1 infection in humans follows a defined pattern with well-characterized features (*1*–*3*); however, the rates of development of disease and the survival times in different individuals vary widely (*4*). The pathogenic potential of the virus (*5*–*8*) and the immunopathogenic effects of the immune response (*9*) have each been postulated to explain the observed differences in progression to disease. One hypothesis that might explain the variable course is that the loss of CD4 T cells in HIV-1–infected individuals is primarily due to increasing antigenic diversity that, beyond a threshold, exceeds the capacity of the immune response to regulate viral population growth (*10*).

To evaluate this hypothesis critically, we directly measured the levels of HIV-1 RNA and tracked viral sequence changes that occurred in concert with the humoral and cellular immune response in samples from a well-defined cohort of HIV-1–infected individuals. Six men with confirmed HIV-1